Modulation of Transcription Factor Ets-1 DNA Binding: DNA-Induced Unfolding of an α Helix

Jeannine M. Petersen, Jack J. Skalicky,* Logan W. Donaldson, Lawrence P. McIntosh, Tom Alber, Barbara J. Graves†

Conformational changes, including local protein folding, play important roles in protein-DNA interactions. Here, studies of the transcription factor Ets-1 provided evidence that local protein unfolding also can accompany DNA binding. Circular dichroism and partial proteolysis showed that the secondary structure of the Ets-1 DNA-binding domain is unchanged in the presence of DNA. In contrast, DNA allosterically induced the unfolding of an α helix that lies within a flanking region involved in the negative regulation of DNA binding. These findings suggest a structural basis for the intramolecular inhibition of DNA binding and a mechanism for the cooperative partnerships that are common features of many eukaryotic transcription factors.

Sequence-specific recognition of DNA by transcription factors is mediated by independent protein modules. The autonomy of DNA-binding domains has recently been challenged by the finding that inhibitory regions, which lie outside functionally defined binding motifs, can alter binding strength or specificity. Deletion mutants of various transcription factors, including TATA-binding protein (TBP), p53, nuclear factor κB (NF-κB), and islet-1 (Isl-1), show enhanced binding activity relative to that of full-length proteins (*1*, *2*). In the cases of TBP and p53, conformational changes also have been linked to the presence of inhibitory sequences (*1*, *3*). Understanding the mechanisms of intramolecular inhibition requires the study of DNA-binding modules within their native structural contexts rather than in isolation.

The *ets* family of transcriptional regulators illustrates this inhibition phenomenon. Members of this gene family are defined by sequence homology within an 85–amino acid region termed the ETS domain (*4*). This region is a minimal DNA-binding domain that forms a winged helix-turn-helix (wHTH) motif (*5*). In at least seven members of the *ets* family, the DNA-binding affinity of the ETS domain is negatively regulated by inhibitory sequences. Inhibition can be released through partial proteolysis or by the formation of complexes with protein partners (*6*–*11*). Models of intramolecular inhibition propose that inhibitory regions can either sterically or allosterically affect the function of the DNA-binding domain. Both mechanisms predict that conformational changes accompany DNA binding. To test for such changes, we performed structural studies on Ets-1, the founding member of the *ets* family.

Ets-1 contains inhibitory regions both NH_2-terminal and COOH-terminal to the ETS domain (*7*–*10*, *12*). Quantitative studies of deletion mutants indicate that inhibition requires both regions (*13*). To examine the structural basis for inhibition, we analyzed repressed (ΔN280) and activated (ΔN331) forms of Ets-1 (Fig. 1A). ΔN331 is the minimal fragment that retains both high solubility during bacterial expression and high-affinity DNA binding. ΔN280 shows characteristics of a structural domain and retains low-affinity binding because both NH_2-terminal and COOH-terminal inhibitory regions are present (*13*, *14*). Both polypeptides were expressed in bacteria and purified protein was used in all studies (*15*). To measure the extent of inhibition, we determined the equilibrium dissociation constants (K_d) of ΔN331 (3.1×10^{-11} M) and ΔN280 (4.4×10^{-10} M) (Fig. 1B). The binding affinities of ΔN280 and ΔN331 for a sequence-specific 21–base pair binding site differed by a factor of 15 (*16*). This lower affinity is similar to that of full-length Ets-1 (*13*). Thus, ΔN280 retains the inhibitory function of native Ets-1.

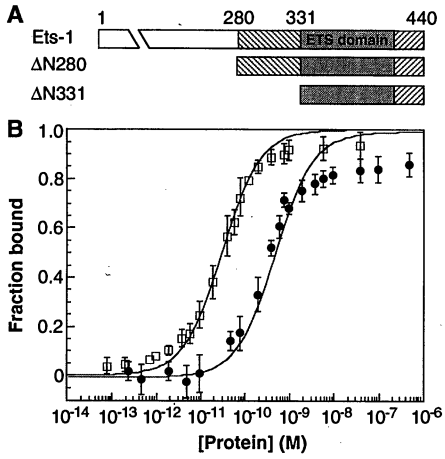

Fig. 1. Equilibrium binding assays demonstrate a ~15-fold difference in affinity (K_d) between ΔN331 and ΔN280 (*16*). (**A**) Schematic representation of full-length Ets-1, ΔN280, and ΔN331. Both fragments retain the native COOH-terminus and the 85–amino acid ETS domain (shaded region). The NH_2-terminal and COOH-terminal inhibitory regions are represented by the striped lines. (**B**) Binding isotherms for ΔN280 (●) and ΔN331 (□). The fraction of DNA bound at each protein concentration was calculated from mobility shift assays. Data points are the average (±SD) of three independent titrations.

The structural origins of DNA-binding inhibition were first investigated by circular dichroism (CD) spectroscopy (*17*). The CD spectra of ΔN331, the fragment that lacks inhibitory function (Fig. 1A), showed no change between 205 and 225 nm upon sequence-specific DNA binding (Fig. 2A). These results suggest that the wHTH motif of Ets-1 assumes the same secondary structure in the bound and free states. This picture is consistent with nuclear magnetic resonance (NMR)–based structures of the ETS domain proteins Fli-1 and Ets-1 that were determined in the presence and the absence of DNA, respectively (*5*). The change in the CD spectra observed between 250 and 295 nm (Fig. 2, A and B) corresponds to a protein-induced alteration of the DNA structure (*18*).

Analysis of ΔN280, the fragment that contains both inhibitory regions (Fig. 1A), provided evidence for the unfolding of the NH_2-terminal inhibitory region upon DNA binding. Addition of DNA to ΔN280 caused a decrease in protein molar ellipticity between 205 and 225 nm (Fig. 2B), which suggests a loss of α-helical secondary structure. This difference cannot be attributed to a change in DNA that is induced by ΔN280 but not by ΔN331, because comparison of the DNA spectra (between 250 and 295 nm) in the presence of ΔN280 or ΔN331 showed identical ellipticity values (Fig. 2E) (*19*). In addition, ΔN280 and ΔN331 make identical contacts to the DNA (*20*). Because there was no difference in ellipticity between bound and free ΔN331 (Fig. 2A), the simplest explanation for the decrease in ΔN280 ellipticity (between 205 and 225 nm) is the loss of α-helical structure in the NH_2-terminal flanking region.

We used partial proteolysis combined with NH_2-terminal sequencing to further define the conformational changes within the Ets-1 polypeptides and to map the region that undergoes a structural transition.

J. M. Petersen and B. J. Graves, Department of Oncological Sciences, Division of Molecular Biology and Genetics, and Huntsman Cancer Institute, University of Utah School of Medicine, Salt Lake City, UT 84132, USA.
J. J. Skalicky, L. W. Donaldson, L. P. McIntosh, Department of Chemistry and Department of Biochemistry and Molecular Biology, University of British Columbia, Vancouver, British Columbia V6T 1Z3, Canada.
T. Alber, Department of Molecular and Cell Biology, University of California, Berkeley, CA 94720, USA.

*Present address: Department of Chemistry, State University of New York at Buffalo, Buffalo, NY 14260–3000, USA.
†To whom correspondence should be addressed.

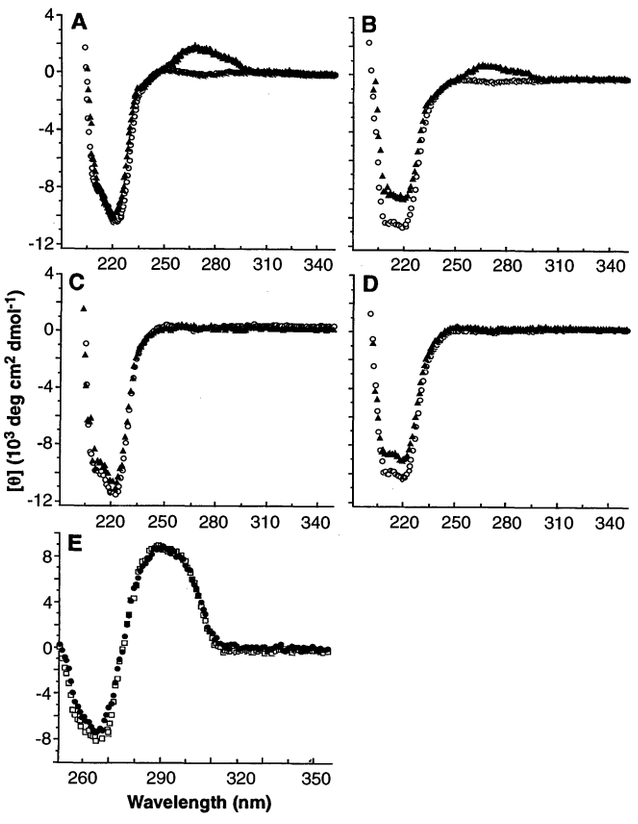

Fig. 2. Normalized CD spectra show that DNA binding is coupled to a loss of secondary structure in the inhibitory region of ΔN280 (*17, 18*). All CD spectra are represented in units of mean residue ellipticity, [θ]. (**A**) ΔN331, the high-affinity fragment, alone (○) and in the presence of specific DNA (▲). (**B**) ΔN280, the fragment containing the inhibitory regions, alone (○) and in the presence of specific DNA (▲). (**C**) ΔN331 alone (○) and in the presence of nonspecific DNA (▲). (**D**) ΔN280 alone (○) and in the presence of nonspecific DNA (▲). (**E**) Comparison of specific DNA in the presence of ΔN280 (●) and ΔN331 (□) (*19*).

Chymotrypsin and trypsin were used in these studies because both Ets-1 polypeptides contain potential cleavage sites scattered throughout their length (Fig. 3A). ΔN280 and ΔN331 were exposed to a fixed concentration of protease in the presence and absence of cognate DNA (*21*). The DNA-binding domain in ΔN331 was resistant to proteolytic cleavage under these conditions (Fig. 3B). Consistent with the CD analyses, the protease studies detected no structural rearrangement of the ETS domain or the COOH-terminal sequences upon DNA binding. In contrast, ΔN280 showed enhanced proteolytic sensitivity in the presence of specific DNA. Both trypsin and chymotrypsin proteolysis yielded two cleavage products, a major and a minor species (Fig. 3C). Quantitation of the trypsin fragments showed that only 8% of free ΔN280 was cleaved during the 10-min incubation interval, compared with 84% of bound ΔN280 (*21*). These data demonstrate that DNA binding stabilized an altered conformation of ΔN280 that exhibited enhanced susceptibility to proteolytic attack.

NH_2-terminal sequencing of the cleavage products (Fig. 3A) showed that trypsin cleaved after residues Arg^{309} and Arg^{311} whereas chymotrypsin cleaved after residues Phe^{304} and Tyr^{307} (*22*). These cleavage sites all lie within the NH_2-terminal inhibitory region. Thus, the conformational change was localized to the NH_2-terminal inhibitory sequences rather than the DNA-binding domain or the COOH-terminal region. These findings are consistent with the CD analyses that suggested that the sequences present in ΔN280, but not those in ΔN331, undergo a loss of α-helical structure upon DNA binding.

Similar experiments were used to examine structural changes induced by protein binding to a DNA duplex that lacks an Ets-1 binding site (*23*). Nonspecific DNA added at the same concentration as specific DNA caused only a modest increase in the protease sensitivity of ΔN280 (Fig. 3C). Under these conditions, and assuming an affinity (K_d) in the micromolar range (*24*), only ~35% of the protein would be bound to DNA. However, nonspecific DNA added at concentrations sufficient to ensure 99% protein occupancy converted all of the ΔN280 to the proteolysis-sensitive form (*25*). CD analyses performed in the presence of nonspecific DNA provided similar results; ΔN280 exhibited a decrease in ellipticity that was proportional to the fraction of protein bound to DNA (Fig. 2D) (*17*). These results indicated that both specific and nonspecific DNA can stabilize an altered conformation of the NH_2-terminal inhibitory region of ΔN280. Nonspecific DNA binding had no effect on the structure of ΔN331 in either assay (Figs. 2C and 3B).

The inhibitory region of ΔN280 that becomes hypersensitive to proteolytic cleavage in the presence of DNA spans residues 304 to 311. NMR analysis of ΔN280 indicates that this region (residues 303 to 310) forms an α helix in the free protein (*26*). In the presence of DNA, almost all potential trypsin and chymotrypsin sites in this region became accessible to cleavage (Fig. 3A), which suggests that this helix is unfolded in the bound state. Our CD analyses are also consistent with the unfolding of this α helix. The mean residue ellipticity of ΔN280 decreased by 20% in the presence of DNA; this corresponds to the unfolding of ~11 helical amino acids (of the total 62 NMR-assigned helical residues), in good agreement with the size (eight amino acids) of the metastable α helix.

The similar DNA-binding affinities of ΔN280 and full-length Ets-1 imply that the structural transition observed in ΔN280 also occurs in full-length Ets-1. Indeed, partial proteolysis of full-length Ets-1 in the presence of DNA shows increased trypsin susceptibility only between residues 309 and 312 (*13*). In our model of full-length

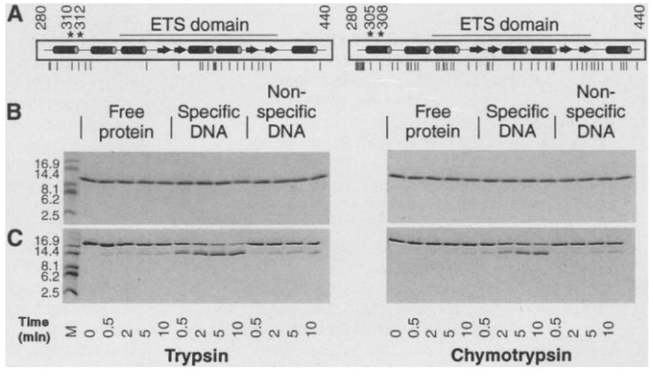

Fig. 3. DNA enhances the protease susceptibility of an α helix within the inhibitory region of ΔN280 (*21*). (**A**) Schematic diagrams of ΔN280 [amino acids 280 to 440 (native terminus)]; α helices and β strands identified by NMR (*26*) are denoted by cylinders and arrows, respectively. The vertical lines designate positions of all possible trypsin (left) and chymotrypsin (right) cleavage sites. The amino acid numbers with asterisks indicate the NH_2-termini of the proteolytic fragments (*22*). (**B**) Proteolysis of ΔN331 alone and in the presence of specific or nonspecific DNA. (**C**) Proteolysis of ΔN280 alone and in the presence of specific or nonspecific DNA. Lane M, molecular mass standards (in kilodaltons).

Ets-1 (Fig. 4), the NH_2-terminal inhibitory region makes intramolecular contacts with the COOH-terminal inhibitory region and the ETS domain in the absence of DNA (*27*). In support of this proposal, NMR studies and modeling of the secondary structure elements of ΔN280 suggest that the two helices within the NH_2-terminal inhibitory region interact directly with the first helix in the ETS domain and the helix in the COOH-terminal inhibitory region, possibly forming a four-helix bundle (*26*). DNA binding allosterically alters these structural elements. Specifically, the α helix at residues 303 to 310 within the inhibitory region unfolds. Refolding restores the repressed state, thereby causing the dissociation of the DNA-protein complex. Stabilization of the derepressed conformation by a partner protein may serve to couple binding to adjacent transcription factors. The localized unfolding could create a hinge that facilitates interactions with the partner. Alternatively, the inhibitory sequences could be the contact surface for the interaction with the partner protein. Thus, inhibition could be relieved by protein-protein interactions within a regulatory pathway.

Our findings demonstrate that Ets-1 contains an inhibitory sequence that becomes disordered upon DNA binding. In contrast to previous studies of transcription factors (*28*), both specific and nonspecific DNA can act as effectors of Ets-1 conformational change. Consequently, sampling of the derepressed conformation can precede specific site recognition. Our results also are distinct from structural and biophysical analyses of specific DNA-protein interactions that implicate local folding as a key to site-specific DNA recognition (*29, 30*). Although many DNA-binding proteins fold upon contact with DNA, our findings provide evidence that the inhibitory region of Ets-1 unfolds upon DNA binding (*31*). This unfolding represents a distinct mechanism for regulating transcription factor activity. Autoinhibitory domains also have been described in kinases, phosphatases, and a calmodulin-dependent Ca^{2+} pump (*32*). Allosterically induced conformational change has been implicated in the derepression of these proteins. Our study of Ets-1 demonstrates that conformational equilibria can also govern the repression and derepression of transcription factor–DNA interactions.

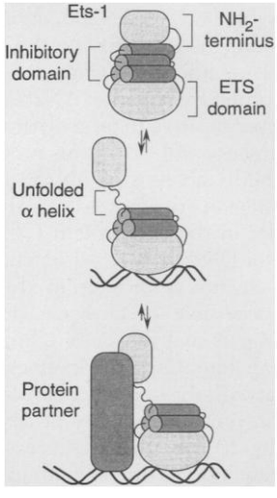

Fig. 4. Model for the allosteric effects of DNA on Ets-1 structure and function. In the absence of DNA, the NH_2-terminal inhibitory region interacts with the ETS domain and the COOH-terminal inhibitory sequences through intramolecular contacts (*26, 27*). The unfolding of an α helix within the inhibitory region accompanies DNA binding and transiently relieves inhibition. The unfolding of the inhibitory region could also expose a putative protein-protein interaction domain. This altered conformation could be stabilized by a protein partner such that the ETS domain of Ets-1 attains high-affinity interactions with DNA.

Note added in proof: The Bam HI–DNA complex has recently been solved by crystallography (*33*). The structure reveals that an ordered α helix at the COOH-terminus of the free protein unfolds upon DNA binding.

REFERENCES AND NOTES

1. P. M. Lieberman, M. C. Schmidt, C. C. Kao, A. J. Berk, *Mol. Cell. Biol.* **11**, 63 (1991); T. R. Hupp, D. W. Meek, C. A. Midgley, D. P. Lane, *Cell* **71**, 875 (1992).
2. S. Grimm and P. A. Baeuerle, *Biochem. J.* **290**, 297 (1993); I. Sanchez-Garcia, H. Osada, A. Forster, T. H. Rabbitts, *EMBO J.* **12**, 4243 (1993).
3. R. Kuddus and M. C. Schmidt, *Nucleic Acids Res.* **21**, 1789 (1993); T. D. Halazonetis, L. J. Davis, A. N. Kandil, *EMBO J.* **12**, 1021 (1993); J. L. F. Waterman, J. L. Shenk, T. D. Halazonetis, *ibid.* **14**, 512 (1995).
4. F. D. Karim *et al.*, *Genes Dev.* **4**, 1451 (1990); B. Wasylyk *et al.*, *Eur. J. Biochem.* **211**, 7 (1993); K. Macleod *et al.*, *Trends Biochem.* **17**, 251 (1992).
5. L. W. Donaldson, J. M. Petersen, B. J. Graves, L. P. McIntosh, *Biochemistry* **33**, 13509 (1994); in preparation; H. Liang *et al.*, *Nature Struct. Biol.* **1**, 871 (1994).
6. A. Giovane, A. Pintzas, S. Maira, P. Sobieszczuk, B. Wasylyk, *Genes Dev.* **8**, 1502 (1994); R. Janknecht, R. Zinck, W. H. Ernst, A. Nordheim, *Oncogene* **9**, 1273 (1994); S. Dalton and R. Treisman, *Cell* **68**, 597 (1992); K. LaMarco, C. C. Thompson, B. P. Byers, E. M. Walton, S. L. McKnight, *Science* **253**, 789 (1991).
7. J. Hagman and R. Grosschedl, *Proc. Natl. Acad. Sci. U.S.A.* **89**, 8889 (1992).
8. J. A. Nye *et al.*, *Genes Dev.* **6**, 975 (1992).
9. F. Lim *et al.*, *EMBO J.* **11**, 643 (1992).
10. C. Wasylyk *et al.*, *Genes Dev.* **6**, 965 (1992).
11. M. Lopez *et al.*, *Mol. Cell. Biol.* **14**, 3292 (1994).
12. R. J. Fisher *et al.*, *Protein Sci.* **3**, 257 (1994).
13. M. D. Jonsen, J. M. Petersen, B. J. Graves, in preparation.
14. Thermal denaturation of ΔN280 monitored by CD shows a cooperative melting transition with an apparent midpoint of unfolding ~10°C greater than that observed for ΔN331 (J. M. Petersen and B. J. Graves, unpublished results).
15. The ΔN331 expression vector was constructed as follows: A fragment encoding *ets-1* residues 331 to 415 was generated by the polymerase chain reaction (PCR) and cloned into the pAED4 expression vector [D. S. Doering, thesis, Massachusetts Institute of Technology (1992)]. An Nde I site engineered by the 5′ PCR primer provided a methionine codon. The resulting clone was modified such that sequences encoding *ets-1* residues 364 to 415 were replaced with a fragment encoding *ets-1* residues 364 to 440. The ΔN280 expression vector was pET3 [A. H. Rosenberg *et al.*, *Gene* **56**, 125 (1987)]. A DNA fragment encoding *ets-1* residues 286 to 440 was ligated to a synthetic adapter encoding an NH_2-terminal methionine (within an Nde I recognition site) and *ets-1* residues 280 to 285. Both proteins were expressed under the control of a T7 promoter in *E. coli* BL21(DE3);pLysS cells. T7 polymerase expression was induced with 1 mM isopropyl-β-D-thiogalactopyranoside for 1 hour at 37°C. Cells were harvested by centrifugation and lysed by sonification in buffer containing 50 mM tris (pH 7.9), 1 mM EDTA, 1 M KCl, 1 mM dithiothreitol (DTT), and 1 mM phenylmethylsulfonyl fluoride (PMSF). The soluble fraction was cleared by centrifugation, dialyzed into buffer containing 20 mM sodium citrate (pH 5.3), 150 mM KCl, 1 mM DTT, 1 mM EDTA, and 0.2 mM PMSF, and applied to a DEAE-cellulose column (Pierce Chemicals). Both proteins flowed through DEAE-cellulose and were loaded directly onto an S Sepharose column (Pharmacia). Active fractions eluted between 250 and 500 mM KCl. Final purification was done on a Superdex 75 gel filtration column (Pharmacia) equilibrated in buffer containing 20 mM sodium citrate (pH 5.3), 1 mM EDTA, and 500 mM KCl. Purity of >99% was determined by Coomassie blue staining. Electrospray mass spectrometry indicated that both proteins lacked the NH_2-terminal methionine.
16. Equilibrium dissociation constants were determined from binding curves generated by mobility shift assays [C. V. Gunther, J. A. Nye, R. S. Bryner, B. J. Graves, *Genes Dev.* **4**, 667 (1990)]. All binding reaction mixtures contained 25 mM tris (pH 7.9), 6 mM $MgCl_2$, 65 mM KCl, bovine serum albumin (100 μg/ml), 10 mM DTT, 0.5 mM EDTA, and 10% glycerol in a 20-μl volume. Purified ΔN331 or ΔN280 was incubated with a radiolabeled 21-bp synthetic DNA duplex (top strand, 5′-AGGCCAAGCCGGAAGTGT-GTG-3′) (*8*) for 20 min at 4°C. Extinction coefficients were determined for ΔN280 (37,850 M^{-1} cm^{-1}) and ΔN331 (29,610 M^{-1} cm^{-1}) as described [S. C. Gill and P. H. von Hippel, *Anal. Biochem.* **182**, 319 (1989)]. Protein concentrations were measured spectrophotometrically at 280 nm. The total protein concentration was corrected for the fraction of active protein (>90% activity for both ΔN331 and ΔN280) as determined by DNA titration experiments. Free DNA and DNA-protein complexes were quantitated by PhosphorImager analysis (Molecular Dynamics, Sunnyvale, CA). Data fit to the equation $[PD]/[D_t] = 1/(1 + \{K_d/[P]\})$ (Kaleidagraph, Abelbeck Software) resulted in K_d values of $3. 1 \times 10^{-11}$ M for ΔN331 and 4.4×10^{-10} M for ΔN280 ([PD] = complex concentration, $[D_t]$ = total DNA concentration, [P] = free protein concentration). In all binding reaction mixtures the DNA concentration was sufficiently low (2×10^{-12} M) to ensure that free protein was approximately equal to total protein.
17. All spectra were collected in 50 mM KPO_4 (pH 7.9), 65 mM KCl, and 0.1 mM EDTA at 4°C on an AVIV 62DS spectrophotometer. All spectra were recorded in a double-chamber mixing cuvette (Hellma, path length 0.874 cm) as follows: First, protein only was added to a single chamber and the spectrum was recorded. Then, DNA (*16, 23*) was added to the second chamber and a spectrum of the unmixed protein and DNA was recorded. Finally, the cuvette was inverted to mix protein and DNA samples and a final spectrum was recorded. To derive protein-only spectra in the presence of DNA (Fig. 2, A through D), we subtracted the free DNA spectra (derived from the unmixed protein and DNA spectra) from the mixed protein-DNA spectra. To obtain DNA-only spectra (Fig. 2E), we subtracted the free protein spectra from the mixed spectra. After each CD spectrum was recorded, samples were left in the mixing cuvette and checked for aggregation as detected by ultraviolet light scattering. The protein concentration was determined before and after addition of DNA by Bradford assay (Bio-Rad) to check for precipitation; neither aggregation nor precipitation was observed. Data were collected in 0.5-nm or 1-nm wavelength steps with averaging times of 10 s from 250 to 190 nm and 3 s from 350 to 250 nm. Concentrations of specific DNA ensured 99% protein occupancy (Fig.

2, A and B). On the basis of a K_d for nonspecific DNA binding in the 10^{-4} to 10^{-6} M range (*24*), the protein occupancy was estimated to be 36% for ΔN331 and 27% for ΔN280 (Fig. 2, C and D).
18. DNA-only spectra of mixed DNA-protein samples containing specific DNA and either ΔN331 or ΔN280 show a difference in molar ellipticity between 250 and 295 nm as compared to the spectra of free DNA, which suggests a protein-induced change in the DNA. This difference was not observed in ΔN280 or ΔN331 samples mixed with nonspecific DNA (Fig. 2, C and D) (J. M. Petersen and B. J. Graves, unpublished results).
19. Specific DNA-only spectra in the presence of ΔN331 and ΔN280 were compared between 250 and 295 nm because ΔN331 and ΔN280 make no important contributions to their CD spectra in this region (Fig. 2, A through D). In contrast, specific DNA shows a strong CD signal in this region (Fig. 2E).
20. The NH_2-terminal deletion mutant ΔN336 and full-length Ets-1 show identical DNA contacts in protection and interference assays (*8*). DNA-binding studies of ΔN331 and ΔN280, including deoxyribonuclease I footprinting and binding site size selection, also indicate identical contact regions (Q. Xu and J. M. Petersen, unpublished results).
21. A time course of protease digestion was performed with fixed concentrations of trypsin (115 ng) or chymotrypsin (215 ng) in a buffer containing 50 mM KPO_4 (pH 7.9), 65 mM KCl, and 0.1 mM EDTA. Proteases were inactivated with 50 mM PMSF, 2% SDS, and 100 mM DTT. Polypeptides were fractionated on Tricine-SDS polyacrylamide gels [H. Schagger and G. von Jagow, *Anal. Biochem.* **166**, 368 (1987)] and visualized by Coomassie blue staining. Stained bands were quantified by video capture and computer-based densitometric analysis with NIH Image software (version 1.49). The concentrations of specific DNA (*16*) and protein that were sufficient to obtain 99% protein occupancy were 10 μM for reactions containing ΔN280 and 15 μM for reactions containing ΔN331. Nonspecific DNA (*23*) was used at equimolar concentrations relative to specific DNA. On the basis of a K_d for nonspecific DNA binding in the 10^{-4} to 10^{-6} M range (*24*), the protein occupancy was calculated to be 46% for ΔN331 and 35% for ΔN280.
22. Fragments were electroblotted from Tricine-SDS polyacrylamide gels to polyvinylidenefluoride membranes and sequenced by Edman degradation with an Applied Biosystems automated sequencer.
23. A 21-bp synthetic DNA duplex (top strand, 5′-AGGCCTGATTGCCCAATTGTC-3′) was used as the nonspecific control DNA. This duplex lacks the core 5′-GGA-3′ motif required for Ets-1 sequence-specific DNA binding.
24. P. H. von Hippel, A. Revzin, C. A. Gross, A. C. Wang, *Proc. Natl. Acad. Sci. U.S.A.* **71**, 4808 (1974).
25. J. M. Petersen and B. J. Graves, data not shown.
26. J. J. Skalicky, J. M. Petersen, L. W. Donaldson, B. J. Graves, L. P. McIntosh, in preparation.
27. The interaction between the NH_2-terminal and COOH-terminal inhibitory regions is supported by the finding that the pattern of protease digestion within the NH_2-terminal inhibitory region is altered in the absence of the COOH-terminal inhibitory region (*13*).
28. J. A. Lefstin *et al.*, *Genes Dev.* **8**, 2842 (1994); R. V. Talanian *et al.*, *Science* **249**, 769 (1990); S. Tan and T. J. Richmond, *Cell* **62**, 367 (1990).
29. M. A. Weiss *et al.*, *Nature* **347**, 575 (1990); V. Saudek *et al.*, *Biochemistry* **30**, 1310 (1991); T. E. Ellenberger, C. J. Brandl, K. Struhl, S. C. Harrison, *Cell* **71**, 1223 (1992); J. D. Shuman, C. R. Vinson, S. L. McKnight, *Science* **249**, 771 (1990); D. Zhao, C. H. Arrowsmith, X. Jia, O. Jardetzky, *J. Mol. Biol.* **229**, 735 (1993); Z. Otwinowski *et al.*, *Nature* **335**, 321 (1988); N. D. Clarke, L. J. Beamer, H. R. Goldberg, C. Berkower, C. O. Pabo, *Science* **254**, 267 (1991).
30. R. S. Spolar and M. T. Record Jr., *Science* **263**, 777 (1994).
31. Because the wHTH motif of Ets-1 does not change secondary structure upon DNA binding (*5*), we predict that the change in heat capacity ($\Delta C°_{assoc}$) that accompanies Ets-1 DNA binding will be affected by the unfolding of the α helix (residues 303 to 310). We propose that $\Delta C°_{assoc}$ will be smaller in magnitude than the values observed for protein-DNA interactions that display a substantial induced fit or rigid body association (*30*).
32. B. E. Kemp and R. B. Pearson, *Biochim. Biophys. Acta* **1094**, 67 (1991); T. R. Soderling, *J. Biol. Chem.* **265**, 1823 (1990); S. Mukherji, D. A. Brickey, T. R. Soderling, *ibid.* **269**, 20733 (1994).
33. M. Newman, T. S. Strzelecka, L. F. Dorner, I. Schildkraut, A. K. Aggarwal, *Science* **269**, 656 (1995).
34. We thank D. King for mass spectrometry analyses, use of equipment, and helpful discussions; B. Schackmann for peptide sequencing; and W. Sundquist and H. Nelson for critical comments on the manuscript. Supported by grants from NIH (GM 38663 to B.J.G.; CA 42014 to the Utah Cancer Center; GM 48958 to T.A.), and the National Cancer Institute of Canada, with funds from the Canadian Cancer Society (to L.P.M.).

31 May 1995; accepted 14 August 1995

A Specialized Pathway Affecting Virulence Glycoconjugates of *Leishmania*

Albert Descoteaux,* Ya Luo, Salvatore J. Turco, Stephen M. Beverley†

For virulence and transmission, the protozoan parasite *Leishmania* must assemble a complex glycolipid on the cell surface, the lipophosphoglycan (LPG). Functional complementation identified the gene *LPG2*, which encodes an integral Golgi membrane protein implicated in intracellular compartmentalization of LPG biosynthesis. *lpg2*$^-$ mutants lack only characteristic disaccharide-phosphate repeats, normally present on both LPG and other surface or secreted molecules considered critical for infectivity. In contrast, a related yeast gene, *VAN2/VRG4*, is essential and required for general Golgi function. These results suggest that *LPG2* participates in a specialized virulence pathway, which may offer an attractive target for chemotherapy.

In *Leishmania*, developmentally regulated glycoconjugates are essential during the infectious cycle. LPG, the major cell surface glycoconjugate of promastigotes, is a multifunctional virulence determinant required for development within the fly, resistance to complement in the bloodstream, and establishment of the infection within the macrophage (*1*, *2*). In *L. donovani*, LPG consists of a phosphoglycan polymer of repeating disaccharide-PO_4 units [Gal(β1-4)Man(α1-PO_4-6)] (where Gal is galactose and Man is mannose) attached by means of a glycan core to an unusual phosphatidylinositol (PI)-lipid anchor (*2*). These components occur on other parasite molecules (sometimes with further modifications), and their expression can be constitutive or specific to a particular stage (*2*–*5*).

LPG is experimentally attractive because its biosynthesis can be studied in vitro and *lpg*$^-$ mutants can be readily generated (*6*–*8*). We recently demonstrated the feasibility of functional genetic complementation in *Leishmania* by identification of *LPG1*, which mediates addition of the Gal_f moiety (where "f" indicates furanose) within the LPG glycan core (*9*, *10*). *LPG1* thus represents a class of genes (class I) encoding LPG biosynthetic enzymes. Here, we report a second class of LPG mutants that affect compartmentalization and LPG assembly. These genes are functionally distinct from those affecting protein secretion and glycosylation.

The mutant C3P0 synthesizes a truncated LPG containing only the glycan core and lipid anchor and lacking repeating units (*8*, *11*). A wild-type *L. donovani* cosmid library in the shuttle vector cLHYG was introduced into C3P0, and LPG$^+$ transfectants were recovered by antibody panning (*9*, *10*, *12*). From these, four cosmids

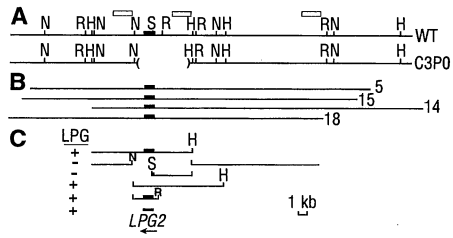

Fig. 1. Functional and physical mapping of *LPG2*. (**A**) Restriction map of the *LPG2* locus. C3P0 contained a deletion (indicated by parentheses) of 6.0 kb containing *LPG2* (black box). Repeating sequences are indicated by shaded boxes. WT, wild type. (**B**) Position of the four overlapping cosmids recovered from LPG$^+$ C3P0 transfectants. (**C**) Localization of *LPG2* by deletional analyses. The indicated restriction fragments were tested for LPG expression after cloning into appropriate *Leishmania* vectors (*13*). N, Not I; R, Eco RV; H, Hind III; S, Spe I.

A. Descoteaux and S. M. Beverley, Department of Biological Chemistry and Molecular Pharmacology, Harvard Medical School, 240 Longwood Avenue, Boston, MA 02115, USA.
Y. Luo and S. J. Turco, Department of Biochemistry, University of Kentucky Medical Center, 800 Rose Street, Lexington, KY 45036, USA.
*Present address: McGill Centre for the Study of Host Resistance, Montreal General Hospital, 1650 Cedar Avenue, Montreal, Quebec H3G 1A4, Canada.
†To whom correspondence should be addressed.